MONITORING OF FLOTATION PROCESSES USING MULTIRESOLUTIONAL MULTIVARIATE IMAGE ANALYSIS (MR-MIA)

J. Jay Liu and John F. MacGregor[1], Carl Duchesne[2], Gianni Bartolacci[3]

[1]*McMaster Advanced Control Consortium, Department of Chemical Engineering, McMaster University, Hamilton, ON. Canada*
[2]*Département de génie chimique, Université Laval, Québec, QC, Canada*
[3]*COREM, 1180, rue de la Minéralogie, Québec, QC, Canada*

Abstract: This paper provides a novel machine vision solution based on multiresolutional multivariate image analysis (MR-MIA) for monitoring of flotation processes. The approach based on MR-MIA is superior to the contemporary machine vision approaches in terms of efficient analysis of morphological and color information and robustness to lighting conditions. The results show that the MR-MIA based approach provides enough morphological and color information of froth needed to describe different froth status. A PCA model built from the information provided by MR-MIA can provide multivariate control charts, from which the transition as well as steady-state process status can be monitored in real time.

Keywords: Flotation Froth, Machine vision, Multiresolutional Multivariate Image Analysis, Wavelet texture analysis, Wavelet size signature

1. INTRODUCTION

The flotation process is one of the important and standard techniques in the mineral processing industries to separate valuable metals from ore (Mckee, 1991). However, it impossible to monitor and control flotation process through fundamental modeling approaches due to the chaotic nature of the underlying microscopic phenomena based on surface chemistry and surface physics. In addition, state-of-the-art instrumentation technologies are not able to provide reliable on-line sensors or analyzers, measurements of which are essential for automatic monitoring and control.

It is widely known that color and morphology of the froth are closely related to mineral concentrations and process status, respectively. As a consequence, many operations are made by operators based on visual appearance of the froth together with their experience about process trends. For these reasons, over the past decade image analysis has been considered as a potentially key component to the solution to this problem.

The purpose of this paper is to provide a novel solution to the characterization and monitoring of the flotation froth based on multiresolutional multivariate image analysis (MR-MIA) (Liu and MacGregor, 2003). By combining multiresolution analysis (MRA) and multivariate image analysis (MIA), it is possible to analyze the spatial and spectral correlation of images within a single framework (Liu and MacGregor, 2003). The approach based on MR-MIA is totally different from the contemporary research in the sense that it handles morphological and color information of froth images systematically and efficiently. In addition, this approach is inherently robust to image quality or lighting conditions, contrary to most contemporary image analysis approaches.

2. VISUAL FEATURES OF FROTH AND EXTRACTION METHODS

Color and structure of flotation froth are very important visual features in the operation of flotation process. Color is strongly related with the mineral concentration carried by the froth (Bonifazi *et al.*,

1999). The structure of the froth, that is its texture or morphology (bubble's size, distribution and, shape, etc.) is known to indicate various froth characteristics such as degree of mineralization (froth load), stability, and so on (Moolman *et al.*, 1996). Operators usually determine the suitable amount of chemical reagents (i.e., control inputs or manipulated variables) based on those visual features of the froth.

Image analysis based on traditional image processing techniques has been applied to flotation processes in order to monitor the process or to infer mineral concentrations. For estimating mineral concentration, statistical features such as descriptive statistics are calculated from each RGB color channel and multiple linear regression or Partial Least Squares (PLS) are used to construct an inferential model (Bonifazi *et al.*, 1998). HSI (Hue, Saturation, Intensity) or HSV (Hue, Saturation, Value) color models other than RGB model were used in some cases in order to overcome high collinearity among R, G, and B values (Bonifazi *et al.*, 1999). In addition, bubble collapse rate, bubble mobility (speed), and various morphological features (froth bubble size, shape, etc.) were extracted via traditional image analysis methods and used in regression, but the correlation of mineral concentration with morphological features was lower than that obtained with color features (Bonifazi *et al.*, 1999).

The analysis of froth structure has frequently been carried out using segmentation methods, texture analysis methods, and Fourier transform (FT) power spectrum. Morphological features such as bubble diameter, aspect ratio, etc. were calculated for each bubble after segmentation of the froth images into bubbles and then used in estimating mineral concentration (Bonifazi *et al.*, 1999). Many other image-processing techniques were used to enhance the quality of image prior to segmentation. Statistical texture analysis methods such as gray-level co-occurrence matrix (GLCM) and its variations were used to classify the status of different froths based on froth texture in order to monitor flotation processes (Moolman *et al.*, 1995). Power spectrum from 1-D or 2-D Fourier transform (FT) was also used to extract textural feature of the froth (Niemi *et al.*, 1999).

It is clear from the literature that the correlation structure among the color in the RGB images has not been considered in most cases. Although HSI and HSV models have sometimes been used in some cases, they are rather basic approaches to handling the collinearity. Lighting condition is also crucial in analyzing color features but efforts made for removing the effect of different lighting or illumination have been so heuristic or ad-hoc that they could not be easily generalized. In this respect, MIA based on Principal Component Analysis (PCA) provides a better approach than others that have been used in the literature since PCA can easily handle the collinearity (Geladi and Grahn, 1996). Furthermore, it was experimentally verified that some features (e.g., energy and entropy) calculated after applying PCA were illumination-invariant as long as intensity saturation did not occur (Tan and Kittler, 1994).

Wavelet texture analysis (WTA) has been considered as the state of the art in texture analysis for many reasons (Liu and MacGregor, 2003). It outperforms other methods such as GLCM-based methods or FT-based methods (Bharati *et al.*, 2003) and is much more computationally efficient and robust to lighting conditions than segmentation-based methods (Bonifazi *et al.*, 1999). Therefore, MR-MIA would appear to offer an excellent alternative to contemporary image analysis approaches for monitoring and control of flotation process. MR-MIA combines advantages of MIA and MRA (Liu and MacGregor, 2003); it can handle high colinearity in RGB froth images more efficiently than HSI and HSV models and can extract structural feature of froth in a faster and more robust manner than segmentation-based or GLCM-based approaches. An overview of MR-MIA methods for extracting color and structural information from froths is discussed in the next section.

3. VISUAL FEATURE EXTRACTION USING MR-MIA

From the literature, it seems that color information and structural information in the froth are not highly correlated to each other and therefore, MR-MIA II is more preferable than MR-MIA I in this situation since spatial information and spectral information are extracted and processed separately (Liu and MacGregor, 2003); Color features will be extracted in the PCA stage of MR-MIA II and then morphological features will be calculated from WTA of the first score image, which it is almost equivalent to the grayscale version of a RGB image in most cases.

The purpose of image analysis in flotation froth is to extract features, which can indicate status of the process and thus can be used for process monitoring and control. Some of the features may be common to other flotation processes but others are not. This is because each plant can show its unique characteristics depending on the flotation cell used, the mineralogy of the ore used, etc. Furthermore, visual features are clearly subjective, and even operators in the same plant may have different criteria when interpreting the images. Therefore, we based our work on interviews about froth visual features with operators and engineers at the plant (Agnico-Eagle's Laronde plant in Quebec, Canada) where the froth image collection was performed.

3.1 CLEAR WINDOWS AND BLACK HOLES

A clear window is a watery portion of the froth, found on the top of the bubbles, that has almost no mineral content (see Figure 1). Therefore, froths with many clear windows usually have big bubbles, and are usually an indication that the degree of mineralization in the froth is very low. The color of the clear windows is much darker and blacker than other regions such as the tops and valleys of the froth. It is one of three major visual features of froth that

operators at Laronde plant use to determine the state of their operations. On the other hand, one can find black holes when froths are excessively loaded with minerals (see Figure 1). A Black hole is a portion of froth surface, which is so close to the pulp that the pulp can be seen through it. Black holes usually appear when bubbles are extremely small and often provide a warning that the entire froth may collapse.

However, these features have never used for monitoring of flotation processes in the literature. Extracting clear windows and black holes can be easily done using masking in MIA since it extracts spectral (i.e., color) features independent of their spatial location. The total areas (i.e., a number pixels) of clear windows and black holes are then easily extracted. The only difficulty is that clear windows and black holes are spectrally similar (i.e., similar colors), and hence difficult to distinguish by MIA alone.

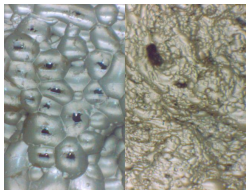

Figure 1 A composite image containing clear windows (left half) and black holes (right half)

Calculating Area of Clear Windows and Black Holes using MIA Masks. A density score plot is one of major analysis tools of MIA; Pixels having very similar spectral features lie close to one another in the score plots, regardless of their positions in the image space and such score plots can be thought as two-dimensional histograms if segmented into a number of bins. An example of a scatter score plot is shown in Figure 2 for the image in Figure 1 where the brightness of each point indicates the number of pixels falling within a bin in the score plot. We can detect different features in the original image space using a density score plot by defining a mask or a feature boundary for each feature as determined from a training image, because the coordinate of each pixel in the score plot is uniquely determined by its variable correlations (Bharati and MacGregor, 1998). The number of pixels within the feature boundaries represents the area of these features in the image space. A feature boundary is usually found by interactive inspection between such score plots and the original image. The feature boundary of clear windows and black holes for the composite image is shown in Figure 2 and pixels falling inside the boundary are highlighted in Figure 2.

3.2 FROTH BUBBLE SIZE

Bubble Size in the froth is one of the most commonly used morphological features throughout the literature and it is another major feature used by operators at the Laronde plant for characterizing process status. In fact, the measurement of froth size has been of great interest in the mining process industry as well as in the literature since it has been extensively reported that the performance of flotation process is strongly related to the size of froth (Moolman *et al.*, 1996).

We can find a size of a bubble, count the number of bubbles, and calculate a histogram of bubble size from them after segmenting each bubble. The biggest problem in using segmentation techniques in practice however is that segmentation is too sensitive to lighting conditions and segmentation techniques used (Bonifazi *et al.*, 1999) and in addition it is computationally demanding compared to other alternatives.

On the other hand, it has been also reported that the froth texture is a strong indicator of process performance (Moolman *et al.*, 1995, 1996). For this reason, statistical texture analysis techniques such as gray-level co-occurrence matrix (GLCM) and its variants have been used to classify froth images into predefined classes that correspond to different process status. Also, fractal analysis has been used in the same context (Hargrave and Hall, 1997). These approaches seem robust to lighting conditions due to the inherent robustness of statistical texture analysis techniques. However, it is difficult to characterize actual froth structure or morphology by using textural features calculated in these methods since textural features and corresponding visual features are not directly related to froth structure such as bubble size (Moolman *et al.*, 1995).

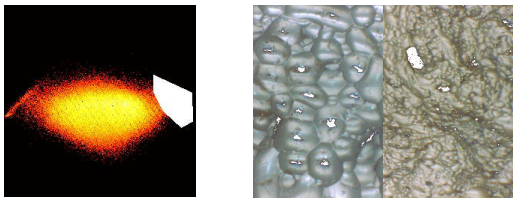

Figure 2 A t_1-t_2 score plot of the composite image with the mask for clear windows and black holes (left) and the composite image where clear windows and black holes found by the boundary are highlighted in white (right)

Calculating Histogram of Froth Bubble Size using Wavelet Size Signature. A basic idea of wavelet texture analysis (WTA) is to extract a textural feature from wavelet coefficients at each resolution and assume that each texture has its unique distribution of features over all the resolutions. Therefore, different textures will have different features if the frequency spectrum is decomposed appropriately. Typical textural features in WTA are energy, entropy, or averaged l_1-norm. However, these WTA features have the same problem; they have no morphological meaning. For this reason, we develop a new feature called wavelet size signature, which can provide a histogram of froth bubble size.

Space-Frequency Representations and Uncertainty Principle. The coefficients of 1-D discrete wavelet transform (DWT) of $f(x)$ can be computed as

$$a_{(j)}[l] = \left\langle f[k], \phi_{j,l}[k] \right\rangle \text{ and } d_{(j)}[l] = \left\langle f[k], \psi_{j,l}[k] \right\rangle, \quad (1)$$

where the $a_{(j)}$'s are expansion coefficients of the scaling function or approximation coefficients, the $d_{(j)}$'s are the wavelet coefficients or detail coefficients, and with some suitable sequence $h[k]$,

$$\phi_{j,l}[k] = 2^{j/2} h[k - 2^j l] \text{ and } \psi_{j,l}[k] = 2^{j/2} g[k - 2^j l] \quad (2)$$

where $g[k] = (-1)^k h[1-k]$. We can easily achieve 2-D DWT by using *separable* scaling functions and wavelets (Vetterli. and Kovačević, 1995). The resulting coefficients are often called *subimages* (the wavelet coefficients are also 2-D) and at each decomposition level j, two-dimensional wavelet transform yields one approximation subimage $a_{(j)}$ and three (horizontal h, vertical v, and diagonal d) detail subimages $d^k_{(j)}$ ($k = h, v, d$).

If we define the durations of signal $f(x)$ in space x and frequency ω by

$$\Delta_x^2 = \int_{-\infty}^{\infty} x^2 |f(x)|^2 dx \text{ and } \Delta_\omega^2 = \int_{-\infty}^{\infty} \omega^2 |F(\omega)|^2 d\omega, \quad (3)$$

respectively then one can define so called a tile in the space-frequency plane. This space-frequency tile tells us the resolutions of wavelet bases in space and frequency domains. Due to the scaling, wavelets used in the decomposition have varying space and frequency resolutions; the frequency duration goes up by 2^j and the spatial duration goes down by 2^j and vice versa. This suggests that the product of space and frequency durations of a signal, i.e., the area of a tile in the space-frequency plane of wavelet transform is a stable quantity and the Uncertainty Principle makes these statements precise, and gives a lower bound for the product.

Wavelet Size Signature. The constant tiling area in the space-frequency tiling of wavelet transform makes it ideally suited for analyzing natural signals. For identifying different size of froth using wavelet analysis froth bubbles with larger sizes will be identified by wider and lower-frequency wavelets and appear in subimages with lower frequency. Froth bubbles with smaller sizes will be identified by narrow and high-frequency wavelets and appear in subimages with higher frequency. At each subimage froth whose (vertical or horizontal) diameters fall within the corresponding width of a tile in the spatial domain will appear. Therefore, the width of a tile in spatial domain can be interpreted as a range of (vertical or horizontal) diameters of bubbles appearing at the corresponding subimage.

If we threshold a subimage then the area of the remaining parts can be thought as the total area of bubbles with sizes corresponding to the subimage. The area can be calculated simply as the fractional the number of thresholded signals (i.e., pixels) at a subimage. Let A_S's be total area of froth at a subimage S calculated from the thresholded subimages and A_T be the area of the entire scene depicted in the original image. Wavelet size signature consists of the fractional areas F_S, which is by its definition

$$F_S = A_S / A_T \quad (4)$$

The average area of a single bubble at a subimage S can be calculated as $\frac{\pi}{4} D_{H,S} D_{V,S}$ where $D_{H,S}$ and $D_{V,S}$ are horizontal and vertical average diameters of a froth calculated from the range of diameters satisfying the space-frequency tiling of DWT and Uncertainty Principle. N_S, the total number of bubbles in the froth with size of $D_{H,S}$ and $D_{V,S}$ in a subimage S can be calculated from wavelet size signature F_S as

$$N_S = \frac{A_T F_S}{\frac{\pi}{4} D_{H,S} D_{V,S}} \quad (5)$$

Therefore, we can calculate a histogram of bubble size from wavelet size signature without requiring actual measurement of froth morphology because A_T is constant for all images. The examples of bubble size histogram calculated from wavelet size signature are shown in Figure 3 Three froth images with different morphological features in Figure 3(b) can easily be discriminated by comparing their histograms in Figure 3(a) as shown in the figure.

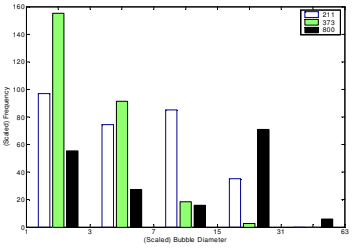

(a)

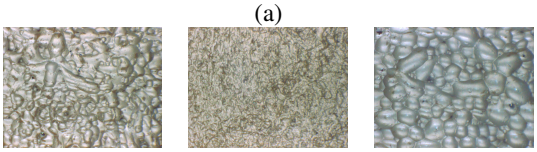

211 373 800

(b)

Figure 3 Illustration of (a) bubble size histograms calculated from wavelet size signature of (b) three different images.

4. DESCRIPTION OF THE FLOTATION PROCESS AND DATA ACQUISITION

The flotation unit in Agnico-Eagle's Laronde plant consists of 3 tank cells used for conditioning and a flotation column. The fresh feed from the grinding circuit enters the first conditioning cell, where lime and activator are added. Lime is used to adjust and control pH. The collector is added in the second conditioning cell. The last conditioning cell is used for mixing only. Air is finally added just before the pulp enters the flotation column. The pulp fresh feed rate was kept nearly constant during all the tests.

The camera was installed on top of the flotation column. It samples 24-bit, 720×480 color images at every minute. We collected images during two plant

tests carried out in two different days. The duration of the step input signals was long enough to ensure the process reached new steady states.

5. FROTH FEATURE EXTRACTION USING MR-MIA II

An MIA model (i.e., loading vectors and a mask for clear windows and black holes) is developed from the composite image used in Figure 2, and used as a global model for the sequence of all images.

As mentioned earlier, clear windows and black holes are spectrally similar although they represent two independent process events. From prior knowledge about the process, the two features are correlated with very different froth morphological features and never really occur together. Therefore it is assumed that in any image, if pixels fall under the mask in Figure 2, they will be exclusively clear windows or black holes. To decide which class they represent, a classical two-class classification problem is formulated with wavelet size signature employed as feature inputs and it is solved using Fisher linear discriminant analysis (Duda *et al.*, 2000).

After calculating the first score image, WTA is applied to the first score image of each image in order to extract wavelet size signature. The decomposition level is chosen to be 6 and symlet wavelets with order 4 are used for all images. A fractional area is calculated only from an approximation subimage at each decomposition level and wavelet size signature is calculated from the difference in fractional areas between every two adjacent levels. By using only approximation subimages, the wavelet size signature of an image is a (5×1) vector. The example of the wavelet size signature is already shown in Figure 3.

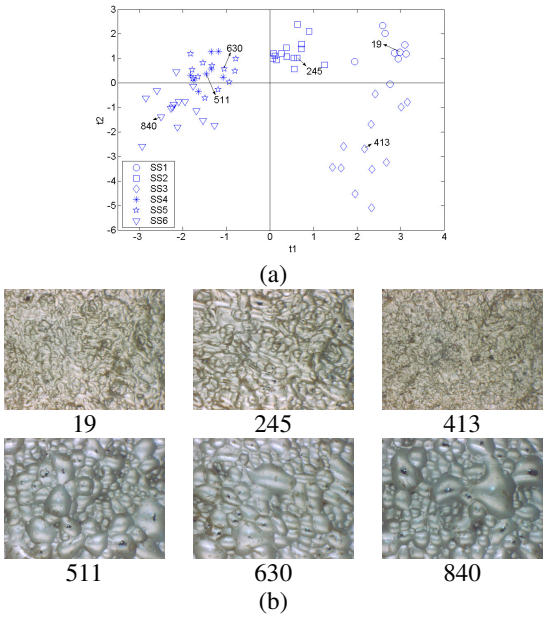

Figure 4 (a) A t_1-t_2 score plot from PCA analysis of MR-MIA II feature variables of selected steady-state images and (b) sample images from 6 steady states.

6. DEVELOPMENT OF PROCESS MONITORING CHARTS

After each (7×1) feature vector (clear windows (1×1), black holes (1×1) and a bubble size histogram (5×1)) is extracted from all images using MR-MIA II, steady state data are selected and a PCA model is built from feature vectors of the selected data. There are 6 steady states (denoted as SS1 ~ SS6 in the legend of figure) corresponding to plant step tests in the data and these steady states form 5 distinct clusters in a t_1-t_2 score plot as shown in Figure 4(a). SS4 and SS5 form one cluster and other steady states form one cluster each and this can be verified by comparing two sample images of SS4 and SS5 in Figure 4(b); they are similar to each other but completely different from 19, 245, 413, and 840 in terms of size of bubbles and area of clear windows. Starting from the fourth quadrant, froth status gradually changes counter clockwise in Figure 4(a). The sample image of SS3 has many small bubbles and some black holes, and the size of bubbles is getting bigger and bigger as one moves counter clockwise. In SS6 in the third quadrant, big bubbles and clear windows are dominant compared to the other 4 clusters. Compared to SS4 and SS5, SS6 has several bigger bubbles and larger area of clear windows. These behaviors in a score plot are verified by a corresponding p_1-p_2 loading plot.

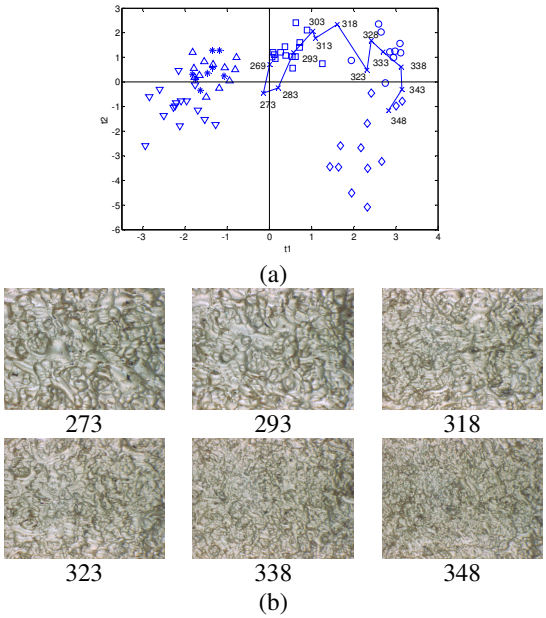

Figure 5 (a) Process transition (from SS2 to SS3) captured by the score plot in Figure 4(a) and (b) selected images during the transition

The process status during the transient states can easily be captured by the same PCA model. Predicted t_1 and t_2 score values of transient data from SS2 to SS3 are plotted over the score plot in Figure 4(a) and shown in Figure 5(a). Six selected images during the transition are shown in Figure 5(b). Starting from the SS2 region, process passes the third quadrant (273 has several clear windows) and comes back to the SS2 region (compare 293 and 245 in Figure 4(b).

They are almost identical.). Then the process moves from SS2 to SS1, passes through the SS1 region, and finally reaches to SS3. These movements can be verified by comparing 6 images in Figure 5(b) and 6 images in Figure 4(b). A process monitoring chart can be easily developed from this score plot. Usually pre-labeled classes are used in the flotation literature on monitoring and control of flotation process but those classes are not independent and discrete events as in typical classification tasks such as character recognition. In process industries, there is always continuous progression from one class to another class and flotation process is one example showing this continuous progression. Therefore, the score plot developed in this work is more suitable for monitoring the froth status in a flotation process. The score space shown in Figure 4(a) can be used as a monitoring chart when it is divided into several meaningful sub-regions based on operators experience and flotation principles. Also a residual plot can be drawn from new data and their prediction by the model in order to detect whether new data (i.e., images in this case) show abnormal behaviors. A residual plot, which corresponds to the t_1-t_2 score plot in Figure 5(a), is shown in Figure 6.

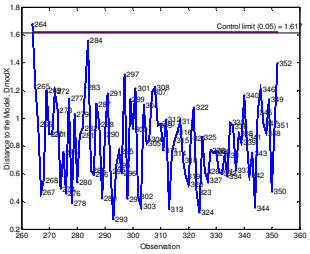

Figure 6. A residual plot corresponding to the t_1-t_2 score plot in Figure 5(a). Upper control limit is from the model built in Figure 4(a).

7. CONCLUSIONS

From the literature on image analysis of flotation process discussed in Sections 2 and 3, we infer that a good image analysis solution should (1) be able to provide rich description of froth morphology, (2) be able to handle correlation in RGB colors, (3) be robust to lighting conditions, and (4) be computationally inexpensive. The proposed approach in this article can satisfy all four requirements whereas contemporary approaches cannot; it can provide rich description of froth morphology compared to approaches based on statistical texture analysis, it is robust to lighting conditions and computationally inexpensive compared to approaches based on segmentation and statistical texture analysis, and it can handle RGB correlation better than approaches based on RGB or HSI/HSV color models.

Monitoring charts developed in this article can provide current froth status no matter whether the process is in a transient or steady state. Estimation of mineral concentration using MIA (Duchesne *et al.*, 2003) can also be done within the same framework of MR-MIA II

REFERENCES

Bharati, M.H., J. Liu, and J.F. MacGregor, (2003). Image Texture Analysis: Methods and Comparisons. Submitted to *Chemometrics and Intelligent Laboratory Systems*.

Bharati, M.H. and J.F. MacGregor (1998). Multivariate image analysis for real-time process monitoring and control. *Ind. Eng. Chem. Res.* **37** (12), 4715-4724.

Bonifazi, G., S. Serranti, F. Volpe, and R. Zuco (1998). Flotation froth characterization by closed domain (bubbles) color analysis. *4th Int. Conf. On Quality Control by Artificial Vision*, Nov. 10-12, Takamatsu, Japan, 131-137.

Bonifazi, G., S. Serranti, F. Volpe, and R. Zuco (1999). Characterisation of flotation froth colour and structure by machine vision. *GEOVISION 99*, May. 6-7, Liege, Belgium.

Duchesne, C., G. Bartolacci, and A. Bouajila (2003). Predicting concentrate grade using multivariate image analysis of flotation froth. *CSChE*, Oct. 26 – 29, Hamilton, Ontario, Canada.

Duda, R.O., P.E. Hart, and D.G. Stork (2000). *Pattern Classification*. 2nd ed. New York: Wiley-Interscience.

Geladi, P. and H. Grahn (1996). *Multivariate Image Analysis*. John Wiley & Sons, Baffins Lane, Chichester.

Hargrave, J.M. and S.T. Hall (1997). Diagnosis of concentrate grade and mass flowrate in tin flotation from colour and surface texture analysis. *Minerals Eng.*, **10** (6), 613-621.

Liu, J. and J.F. MacGregor (2003). Multiresolutional Multivariate Image Analysis and its application to Color Texture Analysis. submitted to *Pattern Recognition*.

McKee, D.J. (1991). Automatic flotation control – a review of 20 years of effort. *Minerals Eng.*, **4** (7-11), 653-666.

Moolman, D.W., C. Aldrich, J.S.J. van Deventer, and D.J Bradshaw, (1995). Interpretation of flotation froth surfaces by using digital image analysis and neural networks. *Chemical Engineering Science*, **50** (22), 3501-3513.

Moolman, D.W., J.J. Eksteen, C. Aldrich, and J.S.J. van Deventer (1996). The significance of flotation froth appearance for machine vision control. *Int. J. Miner. Process.*, **48**, 135-158.

Niemi, A.J., H. Hyotyniemi, and R. Ylinen (1999). Image analysis and vision systems for processing plants. *Proceedings of the 2nd Int. Conf. on Intelligent Processing and Manufacturing of Materials*, **1**, 11-20.

Tan, T.S.C. and J. Kittler (1994). Colour texture analysis using colour histogram. *IEE Proc.-Vis. Image Process.*, **141** (6), 403-412.

Vetterli, M. and J. Kovačević (1995). *Wavelets and Subband Coding*. Englewood Cliffs, NJ: Prentice Hall.